Brain Tumor Segmentation Based on Deep Learning

Hajar Cherguif
LIIAN Laboratory
Department of Informatics Faculty of Sciences Dhar-Mahraz
University of Sidi Mohamed Ben Abdellah
Fez, Morocco
hajar.cherguif@usmba.ac.ma

Jamal Riffi
LIIAN Laboratory
Department of Informatics Faculty of Sciences Dhar-Mahraz
University of Sidi Mohamed Ben Abdellah
Fez, Morocco
riffi.jamal@gmail.com

Mohamed Adnane Mahraz
LIIAN Laboratory
Department of Informatics Faculty of Sciences Dhar-Mahraz
University of Sidi Mohamed Ben Abdellah
Fez, Morocco
adnane_1@yahoo.fr

Ali Yahyaouy
LIIAN Laboratory
Department of Informatics Faculty of Sciences Dhar-Mahraz
University of Sidi Mohamed Ben Abdellah
Fez, Morocco
ayahyaouy@yahoo.fr

Hamid Tairi
LIIAN Laboratory
Department of Informatics Faculty of Sciences Dhar-Mahraz
University of Sidi Mohamed Ben Abdellah
Fez, Morocco
htairi@yahoo.fr

***Abstract*— Brain tumors develop rapidly and aggressively, causing brain damage and can be life threatening. Determining the extent of the tumor is a major challenge in brain tumor treatment planning and quantitative assessment to ameliorate the quality of life of patients. Magnetic resonance imaging (MRI) is an imaging technique widely used to evaluate these brain tumors, but manual segmentation prevented by the large amount of data generated by the MRI is a very long task and the performance is highly dependent on operator's experience. In this context, a reliable automatic segmentation method for segmenting the brain tumor is necessary for effective measurement of the extent of the tumor. There are several image segmentation algorithms, each with its own advantages and limitations. In this paper, we propose a method based on Deep Learning, using deep convolution networks based on the U-Net model. Our method was evaluated on real images provided by Medical Image Computing and Computer-Assisted Interventions BRATS 2017 datasets, which contain both HGG and LGG patients. Based on the experiments, our method can provide a segmentation that is both efficient and robust compared to the manually delineated ground truth. Our model showed a maximum Dice Similarity Coefficient metric of 0.81805 and 0.8103 for the dataset used.**

Keywords*— *Brain Tumor; Segmentation; Deep Learning; Convolution Network; U-Net; Medical Image

I. INTRODUCTION

A brain tumor is defined as a mass of abnormal cells in the brain that can progress to benign and malignant tumors (Fig.1). Brain tumors also differ according to their origin and location. Primary brain tumors are those that develop directly in the brain, whether or not they are cancerous tumors. The most common malignant tumors include gliomas, medulloblastomas [1]. Among benign primary tumors, rarer than malignant primary tumors, include hemangioblastomas, meningiomas, pituitary adenomas, osteomas, pinealomas, and so on [2]. Secondary brain tumors originate from other organs already affected by cancer whose tumor cells have migrated to the brain and multiply there. Among the most common tumors that cause brain metastases [3] : breast cancer, lung cancer, skin cancer (melanoma), kidney cancer, colon cancer, etc. The causes are still poorly understood today when symptoms develop, a radiological examination with a biopsy will be carried out to determine the treatment to be adopted

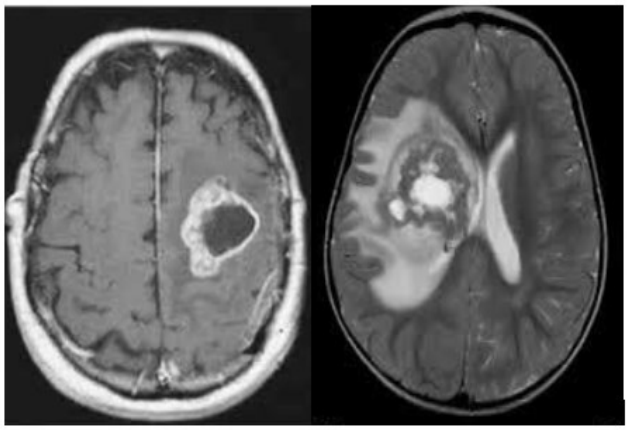

Fig. 1. Benign tumor is on the left and malignant tumor is on the right.

Cancerous or not, a tumor when it grows causes prisions on certain areas of the brain. Depending on the type of tumor and its location, treatment may vary, usually, surgery is used to remove the tumor if it is accessible, and otherwise radiosurgery will be performed if the tumor is malignant [4,5].

For successful surgery, we use segmentation to efficiently detect and segment brain tumors. There are two ways to segment brain tumors. The first one is manual segmentation, which is a subjective decision and does not give the desired results because it is difficult to fully extract brain tumors without damaging surrounding brain tissue, i.e. healthy tissue. Hence, the need for automatic segmentation, the second way, which detects brain tumors quickly and accurately, and is essential for treatment planning and quantitative evaluation. There are also too many approaches to segmenting medical images. We can divide them into three types [6-8]: classical approaches, machine learning approaches and others based on deep learning (Fig.2). In classical approaches, regional approaches aim to locate homogeneous areas of images, marking the presence of regions. On the other hand, contour approaches look for discontinuities of images, characterizing the presence of boundaries between regions. Machine learning, or more precisely clustering, is often used to detect and segment brain tumors. K-means [9] and, GMM [10] are the best known and most used in unsupervised learning because of their simplicity of implementation. In recent years,

978-1-7281-4813-7/19/$31.00©2019IEEE

researchers have tried to find many ways to solve the problem of semantic segmentation of medical images, including CNN [11], FCN [12], and U-Net [13-15]. In this work, we focus on using U-Net according to its best results in terms of segmentation and we will detail it later.

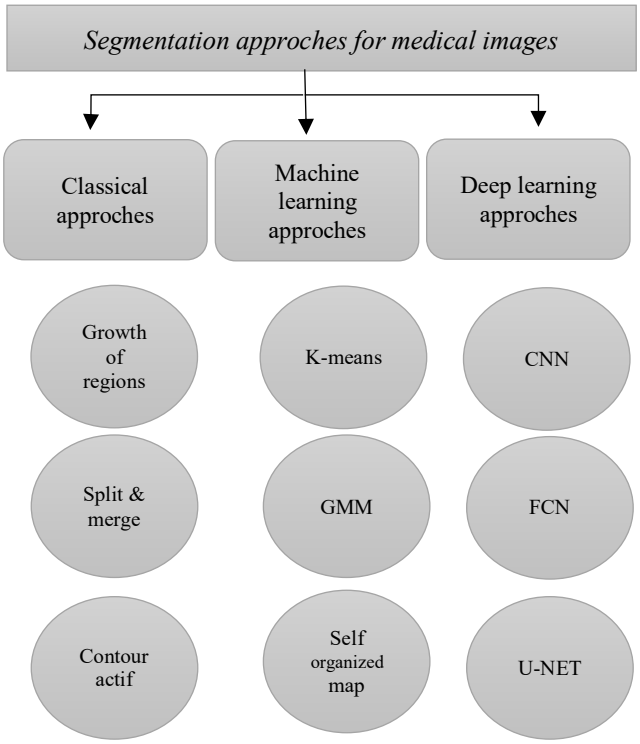

Fig. 2. Approaches used for medical image segmentation.

We are also interested in magnetic resonance imaging (MRI) [16,17], one of the most commonly used imaging modalities, which has become an indispensable tool for any clinical examination such as diagnosis, tumor monitoring and outcome prediction for patients. It is so difficult to locate irregularly shaped tumors with only one modality, so the MRI modalities are combined to produce a multimodal image containing information that can be used for tumor segmentation with significant performance improvement. These modalities are T1-weighted MRI (T1), T1-weighted MRI with contrast enhancement (T1c), T2-weighted MRI (T2) and T2-weighted MRI with fluid-attenuated inversion recovery (Flair) (Fig.3).

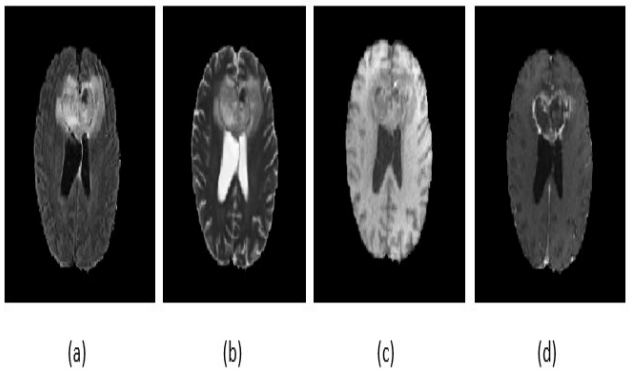

Fig. 3. (a) Flair; (b) T2; (c) T1; (d) T1c.

In this article, we used the U-Net architecture to develop a completely convoluted 2D segmentation network [13]. To adapt to unbalanced samples, we applied a Dice Similarity Coefficient introduced in [18]. The proposed method was validated using the BRATS 2017 datasets. Compared to the truth of the manually delineated ground, our fully automatic method resulted in superior segmentation of the tumor regions. The rest of this paper is organized as follows: in Section 2, we briefly present previous work on the segmentation of brain tumors. Section 3 describes the different steps of our proposed approach and we present some experimental results in Section 4.

II. Related works

Supervised and unsupervised paradigms cover two broad areas of machine learning. In both cases, we are given data, but in one case, we have tagged data and in another, we have unlabeled data. The unsupervised paradigm is much less explored, getting the data is cheap, but getting labels is hard. Supervised learning is the method of the future; it is one of the most interesting open research topics. The paradigm of supervised learning is the dominant paradigm in machine learning and there are a vast amount of articles being written about it, we talk about classification, regression, segmentation and different methods to do supervised learning. Between the two, some techniques do both, supervised and unsupervised. They are called semi-supervised or self-supervised, use an unsupervised learning element, and pair them with supervised learning. In this article, we have reviewed only some of the most relevant studies for the segmentation of brain tumors. An overview and a detailed topical review of different methods of this topic can be found in [19,20].

In recent years, several researchers have shown a growing interest in the development of medical image segmentation algorithms. They proposed semi-automatic and fully automatic methodologies for image segmentation. Unsupervised learning-based [21-26] clustering has been successfully used to segment a brain tumor by clustering data according to certain similarity criteria. To achieve effective and fully automatic segmentation of brain images, Al-Dmour et al. [21] proposed a method that combines semi-supervised and unsupervised classification techniques. This method consists of five main steps: reduce noise using a median filter, eliminate background using a global thresholding technique, use the subtractive clustering method to determine the initial values of the cluster center, generate a membership function from Fuzzy C-Means (FCM), and feed the cluster centers and membership values to the SSSFC algorithm. In [23], an automatic algorithm has been proposed to detect and segment brain tumors scanned by multimodal 3D magnetic resonance image data. The proposed algorithm used a fuzzy c-means clustering cascade algorithm and fused it with a decision support algorithm based on prior information. The proposed framework has been validated on six volumes selected from the BRATS 2012 database, but has unfortunately been tested on a very limited number of data sets. The unsupervised automated brain tumor segmentation method proposed by Juan-Albarracín et al. in [24] consists of four steps: processing anatomical magnetic resonance images, extracting features and reducing dimensionality, unsupervised voxel classification and automatic isolation of tumor classes.

Unlike unsupervised learning [27-32], supervised learning methods require which of the new instances can be classified and then segmented. We must say that these supervised approaches are achieving good results in the field of medical imaging. To feed an Extremely Randomized tree (Extra-Trees), Pinto et al. [29] proposed a fully automatic glioma segmentation method, using both appearance and context-based features defined on the T1c, T2 and Flair MRI sequences. This proposed method was obtained a high score Dice over Brats 2013 database challenge. In the same context, the difference between [29] and [30] is that in the first, the split of trees is deterministic and in the second, it is random. Soltaninejad et al. [30] used an extremely random tree classifier combined with the detection and segmentation of each superpixel for FLAIR MRI images. More recently, Bonte et al. [32] have presented a new method capable of delimiting the different tumor tissues from a minimum amount of data. That is why they combined Random Forests classification with voxelwise texture and abnormal characteristics on a T1 and FLAIR MRI.

Recently, Deep learning methods [33] and convolutional neural networks (CNN) are used to resolve semantic segmentation tasks in computer vision. Semantic segmentation using CNN makes it possible to effectively classify each pixel of the input image. The idea of semantic segmentation is to create a map of the fully detected object areas in the image. There are many methods of deep learning about this subject. We will mention some of them.

The naive approach [34,35] aims to reduce the task of segmentation to that of classification. By converting a normal convolutional neural network used for classification into a fully convolutional neural network used for segmentation, we obtain a form of localization. Despite this, it is still a classification problem because; it is just an assignment of a class to each of the output pixels. The main problem with this approach is the loss of a certain resolution due to reduced activation over a large number of steps. To improve the architecture with multi-resolution layer combinations, Long et al. [12] adapted classification networks such as AlexNet and GoogleLeNet into fully convolutional networks (FCN) and transferred their learned representations by fine-tuning to the segmentation task. Then, they proposed to use the skip-architecture that combined the high-level representation of the deep decoding layers with the appearance representation of the shallow encoding layers to produce a detailed segmentation.

A different approach to solving the problem of semantic segmentation through deep learning is based on a downsampling-upsampling architecture, in which the left and right parts have the same size in terms of the number of parameters that can be formed (trainable parameters). This approach is also named encoder-decoder architecture. The main idea of this approach is to obtain the result (the output image) with the same size of the original image (input image). This can be achieved by saving the information using skip connections or by reserving all layers of convolution and pooling by applying unpooling and deconvolution operations in the decoder part, but at the same location as where convolution and max, mean or average pooling is applied in the convolutional or encoder part of the network. A functional example of such an architecture is the SegNet model presented by Badrinarayanan et al. [36] with an encoder network identical to the 13 convolutional layers of the VGG16 network [37] and a corresponding decoder part. The role of the latter is to map the low-resolution encoder feature maps to full input resolution feature maps for pixel-by-pixel classification. Badrinarayanan et al. [36] compared their proposed architecture with the widely adopted FCN [12] and this comparison reveals the memory/precision trade-off necessary to achieve good segmentation performance.

U-net [13-15] is another model of encoder-decoder architecture. This architecture is divided into three parts: the downsampling part, the bottleneck part, and the upsampling part. The first part, also called the contracting, follows the typical architecture of a convolution network. This path is composed of four blocs. Each block is composed of two three-by-three convolution layer followed by an activation function with/not with batch normalization and a two-by-two max pooling operation. At each contracting tab, the number of feature maps doubles due to pooling. The purpose of this downsampling path is to capture the context of the input image in order to be able to perform segmentation. The bottleneck exists between the downsampling and upsampling paths. This part is constructed from two simple convolutional layers with batch normalization and dropout. The upsampling part that exists in front of the contracting party, called the expansion path, is also composed of four blocks. The only difference between these two parts is that instead of maximum pooling, there is a transposed convolution. The objective of this third side is to allow a precise location combined with contextual information from the contracting part. Thus, each block is composed of a deconvolution layer with stride two, a concatenation with the corresponding characteristic map of the contracting path and two three-by-three convolution layer with an activation function. In total, the network consists of 22 convolutional layers plus one-by-one convolution on the final layer used to map each element of the feature vector according to the desired number of classes. To solve the problem of cell tracking, Ronneberger et al. [13] introduced U-Net architecture. They have formed this end-to-end network from very few images and surpass the sliding-window convolutional network on the ISBI challenge for neural structures segmentation in stacks of electron microscopes. Many researchers have tried to use U-net architecture in several fields. Among these researchers are Dong et al. [15] who have developed a new fully convoluted 2D segmentation network based on the U-Net [13] architecture. They evaluated their method on the BRATS 2015 datasets and used a complete increase in data to improve the accuracy of segmentation.

Encoder-decoder architectures have seemed more effective in these tasks so, we use U-net because of its good performance on different biomedical segmentation applications.

III. Proposed Approch

A. *Description of our model*

In this study, we want to solve the problem of brain tumor segmentation by proposing a new network architecture, based on U-Net [13]. Our network architecture is an encoder-decoder architecture, i.e. it consists of a downsampling path and an up-sampling path as shown in (Fig.4). This architecture is divided into three parts: the contracting part, the bottleneck part, and the expansion part. The contracting path has four convolutional blocks. Each block is composed of three convolutional layers with a three-by-three filter, one-by-one

stride followed by a rectifier (ReLu) activation function with batch normalization. At the end of every block, the max-pooling is applied in this contracting path with a stride of two-by-two, which reduces the size of feature maps from 240×240 to 15×15. Due to the pooling, at each contracting tab, the number of feature maps increase from 1 to 1024. The bottleneck part is composed of three simple convolutional layers with batch normalization and there is no maximum pooling. The expansion path also includes four blocks. Each block starts with a deconvolutional with a three-by-three filter, two-by-two stride, which increases the size of the feature maps twice from 15×15 to 240×240 in both directions but reduces the number of feature maps by two. Unlike the original U-Net architecture [13], we use three convolution layers per block to achieve more efficient brain tumor segmentation, and zero paddings to maintain the output dimension for all convolutional layers of the encoding and decoding path. Finally, one-by-one convolution on the final layer used to map each element of the feature vector according to the desired number of classes. Unlike [15], we did not apply L1, L2 or dropout to the network because there is no significant improvement in performance. The total of the parameters of this network, the trainable parameters, and the non-trainable ones are tabulated in Tab.1.

Tab. 1. Numbers of each parameters setting for the developed U-Net.

Parameters	Value
Total	46,772,929
Trainable	46,755,265
Non-trainable	17,664

B. BRATS 2017 datasets and data augmentation

The proposed method was tested and evaluated on real images provided by Multimodal Brain Tumor Image Segmentation (BRATS) 2017 datasets [38-40], which contain 210 high-grade gliomas (HGG) and 75 low-grade gliomas

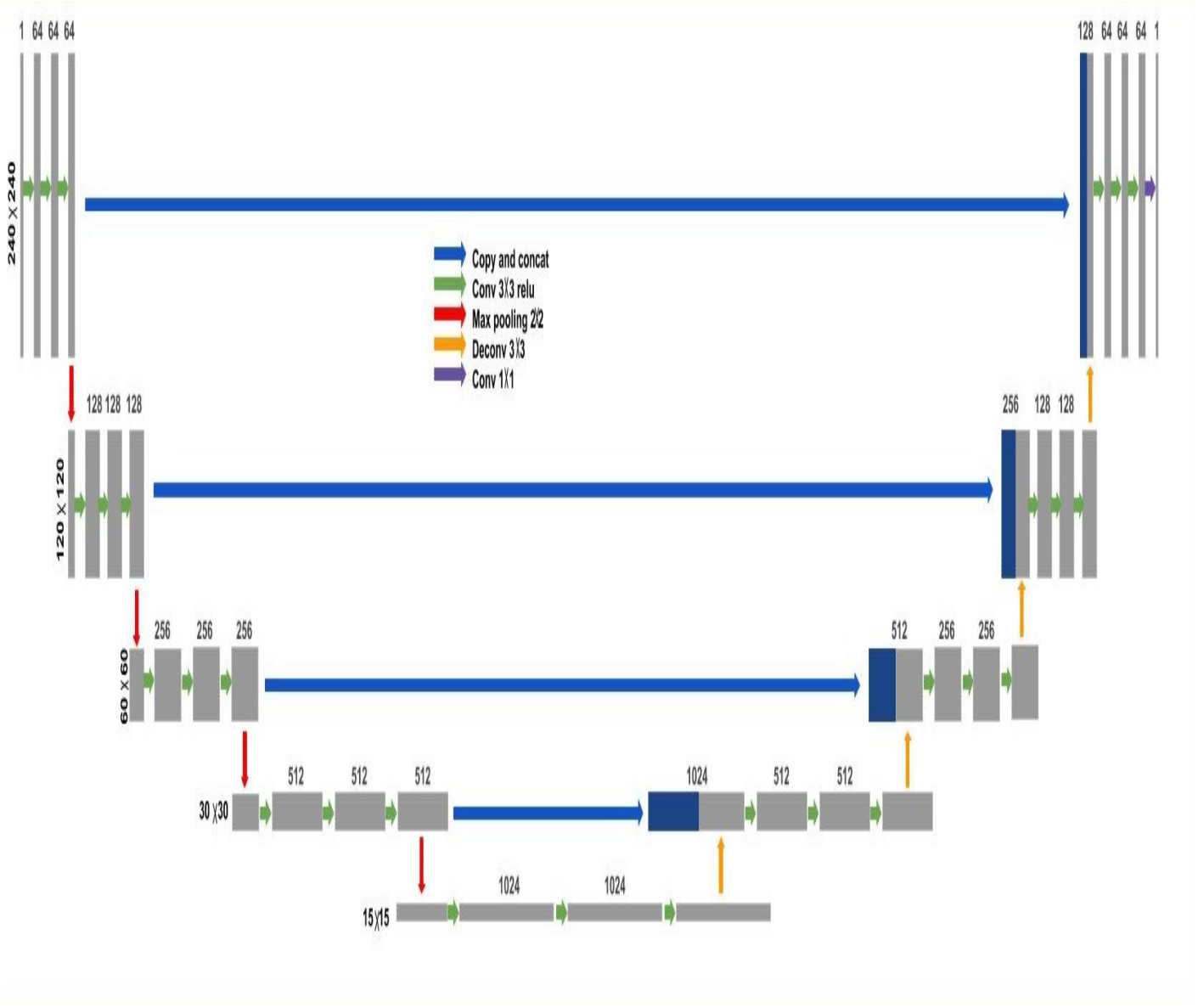

Fig. 4. Our developed U-Net architecture.

(LGG) patients scans. Multimodal MRI data are an essential tool for any clinical examination. Their modalities are combined to produce a multimodal image containing information that can be used for tumor segmentation with significant performance improvement. These modalities are T1 weighted MRI (T1), T1 weighted MRI with contrast enhancement (T1c), T2 weighted MRI (T2) and T2 weighted MRI with fluid-attenuated inversion recovery (Flair) [41] (Fig. 3). Multimodal MRI data were selected for their availability for each patient in the BRATS 2017 datasets. The four MRI sequences are performed using T1, T1c, T2 and FLAIR for each patient and manual segmentations with the four intra-tumoral classes (labels) are available for each case, namely: complete tumor, edema, enhancing tumor, necrosis, and non-enhancing tumor (Fig. 5). In this study, we focus only on the use of FLAIR images to detect and segment the complete tumor, and for this purpose manual segmentations were used as the ground truth in the segmentation model and the final evaluation of segmentation performance.

Inspired by [15], we applied the same set of data augmentation methods because of its ability to improve network performance by producing more and more training data from the original data. This set of data augmentation methods is summarized in Tab.2 includes γ which controls the brightness of the outputs, and (α , σ) controls the degree of the elastic distortion.

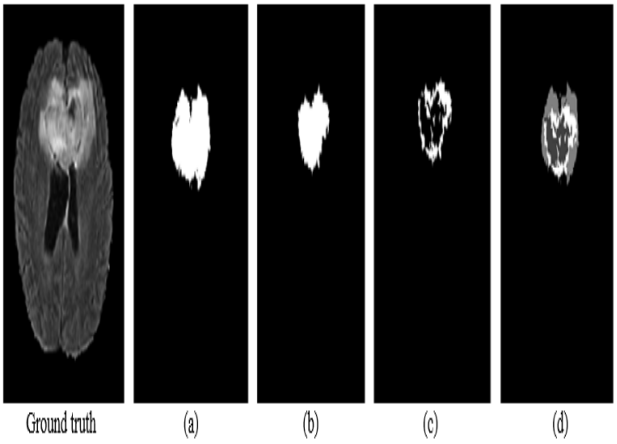

Fig. 5. (a) Full ; (b) Edema ; (c) ET; (d) All

Tab. 2. Summary of the applied augmentation methods

Methods	Range
Flip horizontally	50% probability
Flip vertically	50% probability
Rotation	± 20º
Shift	10% on both horizontal and vertical direction
Shear	20% on horizontal direction
Zoom	± 10%
Brightness	γ = 0.8-1.2
Elastic distortion	α = 720; σ = 24

IV. Evaluation and Experiment results

A. Libraries

The most popular deep learning library in the world today is Google's Tensorflow. In TensorFlow, the model is represented as a data flow graph. The graphic contains a set of nodes called operations. They are computation units, they can be as simple as addition or multiplication and can be a complex multivariate equation. Each operation takes a tensor at the input and a tensor at the output. A tensor is the way data is represented in TensorFlow and flows between operations, hence the name TensorFlow. Although Tensorflow is one of the best libraries on the market for deep learning, but also a little complex, that's why Keras exists. A good reason to choose Keras is that we could use the TensorFlow backend without really learning it. It uses an object-oriented design so that everything is considered an object since layer model optimizers and all model parameters can access the object properties. Our network has been implemented under in Python for its simplicity, elegance and ability to solve complex problems in less time, which has made it grow in the field of deep learning, and also by using the TensorFlow and Keras libraries.

B. Training and Optimization

When it comes to segmentation, it is not easy and trivial to choose the right quality metric or the best cost function. In general, many methods can be applied to form a pixel-wise segmentation model, but each of these cost functions works best on a particular dataset. In the case of medical images, the dice coefficient [18] is a strong choice compared with the cross-entropy function or the quadratic cost function. It is really more efficient for class imbalance problems, which means that some segments occupy fewer pixels or voxels than others.

The DSC (Dice Similarity Coefficient) was used to evaluate the segmentation for each tumoral region. The DSC (provides a measure of the similarity between the manual delineated brain tumoral regions and the results of the segmentation of our fully automatic method, which is

$$\mathbf{DSC} = \frac{2TP}{FP+2TP+FN} \quad (1)$$

in which TP, FP, and FN refer to the measurements of true positive, false positive and false negative respectively.

We have adopted the adaptive moment estimator (Adam) [42] to minimize the cost function with respect to its parameters. Adam usually uses the first and second gradient moments to update and correct the moving average of the current gradients. The first parameter of our Adam optimizer is the learning rate, which defines how fast we want to update our weights. If we choose a high learning rate, our model can skip the optimal solution and if we choose it too small, we will need too many iterations to converge towards the best results. Therefore, we were set the learning rate at 0.0001. The second parameter is the maximum number of epochs and we have set it at 300.

C. Discussion and results

To evaluate the effectiveness of the proposed architecture, we are conducting experiments on the BRATS 2017 dataset, and to demonstrate the robustness of our method, we are comparing it to two different methods based on a U-Net

architecture [13] dedicated to the brain tumor segmentation. For use in this article, we call them respectively U-net_1 (Fig.6) and U-net_2 (Fig.7) architectures for simplicity. The only difference between these two architectures and ours is that, in the first method, we used only one layer for each block. The second had two layers for each block [13]. The number of convolutional and deconvolutional layers for each architecture is presented in Tab.3. The U-Net_1 and U-Net_2 were also evaluated on MICCAI BRATS 2017.

Tab.4 presents the DSC and precision results of the U-Net_1 architecture, the U-Net_2 architecture, and our developed architecture, respectively. Compared to other methods, our method achieved a higher DSC of 0.81 (Fig.10) for complete tumor brain segmentation and an accuracy of 0.99 for the full tumor with the core one, demonstrating that our method obtained superior results for complete tumor segmentations. To see more clearly that, (Fig.8) shows some exemplary qualitative segmentation results compared to the ground truth, and (Fig.9) compares our prediction method with the other two prediction methods. According to the results, our method allows an efficient and robust segmentation against the manually delimited field truth and also gives superior results for the central tumor regions.

Once we fixed the model, the calculation time for prediction is about 2 to 3 s per case. Each validation training session requires approximately 19 hours on an NVIDIA GeForce GTX 1050 with 16 GB of memory, compared to 9 hours for U-Net_1 and 12 hours for U-Net_2 with the same hardware configuration. Compared to our computation time, previous studies were less effective: 30 s [43], 25 s at 3 min [11], and about 8 min [44] to predict a tumor study. Some of the limitations we have encountered in this 2D network, the learning error curve using DICE is a total mess (Fig. 10), it has given us absolutely no information on convergence, so in this regard perhaps the cross-entropy error has given a regular learning error. Despite these limitations, the model developed has nevertheless demonstrated promising segmentation results with efficiency.

To summarize, our objective behind this work was to improve the segmentation of brain tumors and this is by thinking about a method that will be powerful and will give better results. At first, the idea was that the number of convolutional layers per block had some impact on the outcome of brain tumor segmentation or not. And for this reason, we have thought about developing a U-Net architecture with a data augmentation that will contain three convolutional layers per block, unlike the original one [13] which contains only two convolutional layers. We compared our architecture with our two other architectures, the first containing only one convolutional layer per block and the second absolutely inspired by [15]. Experiences have shown that as soon as the number of layers is large the prediction is the same as the truth on the ground (Fig.8) (Fig.9). Under the same conditions, whether it is the hardware configuration of the PC or the error/evaluation metric or the data augmentation methods, our developed architecture allows a more or less perfect segmentation of the complete tumor (accuracy = 0.99). Our method gives us satisfactory results for the detection and segmentation of brain tumors. This work was only a first step in this area, we focused only on the complete tumor, while we wanted to improve our method of detecting other forms such as ET, modify the data augmentation methods to give us a very high DICE value and then decrease the number of epochs.

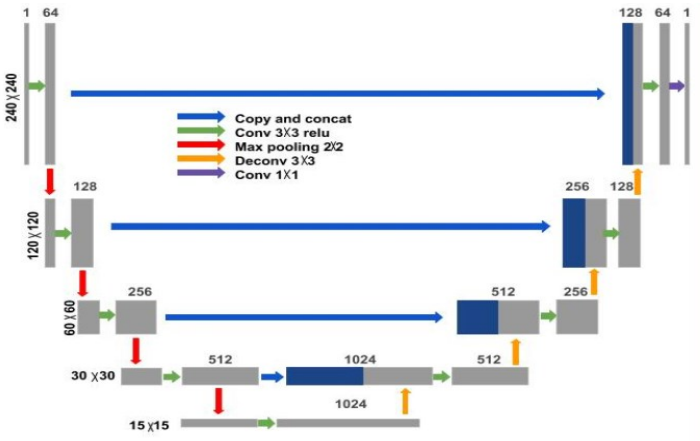

Fig. 6. U-Net_1 architecture.

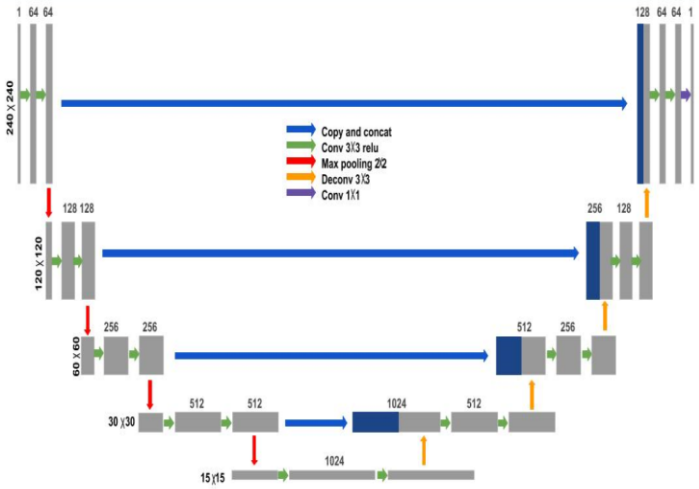

Fig. 7. U-Net_2 architecture.

Tab. 3. Number of layers for each architecture.

Architectures	Number of convolutional layers	Number of deconvolutional layers	Total of layers
U-Net_1	9	4	13
U-Net_2	18	4	22
Ours	27	4	31

Tab. 4. Quantitative results of our proposed fully automatic brain tumor segmentation method compared to the two others methods.

Architectures	Dice_coef	accuracy
U-Net_1	0.65	0.47
U-Net_2	0.72	0.62
Ours	0.81	0.99

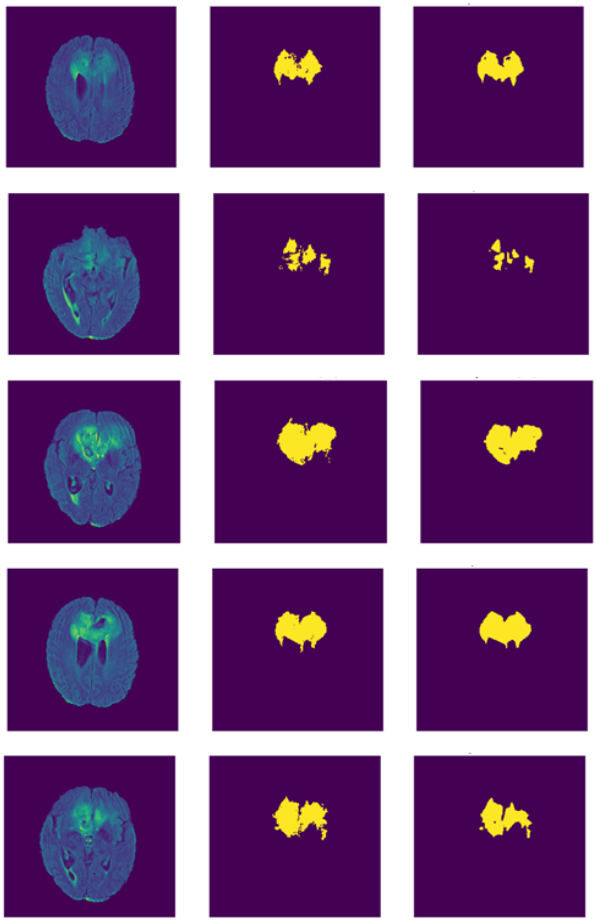

Fig. 8. Segmentation results for the examplar FLAIR images compared with manual delineated ground truth. (a) Flair; (b) Ground truth; (c) Full prediction.

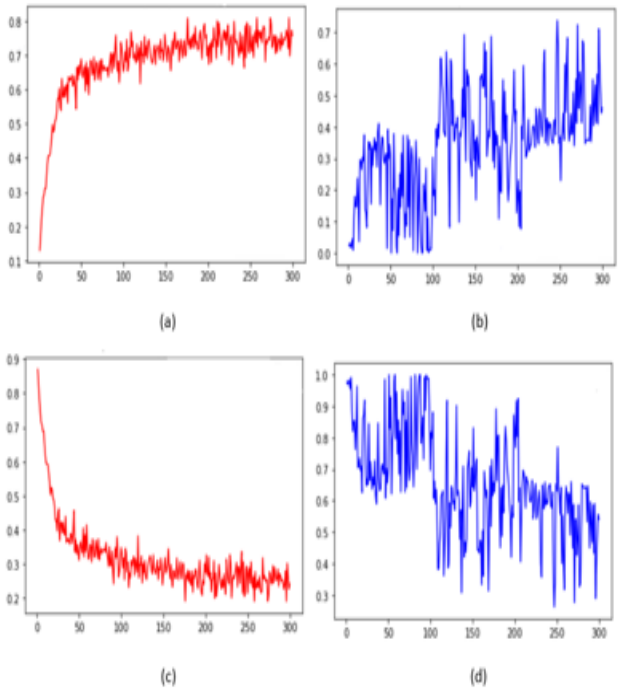

Fig. 10. (a) Learning Accuracy; (b) Validation Accuracy; (c) Learning Error; (d) Validation Error

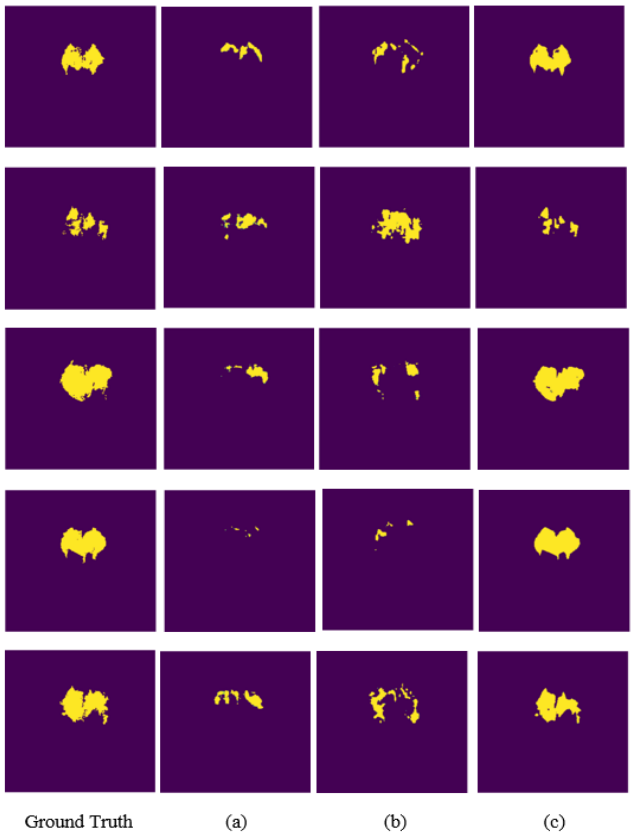

Fig. 9. Segmentation results of our developed architecture and the two other methods for the examplar FLAIR images compared with manual delineated ground truth. (a) Prediction of U-net_1; (b) Prediction of U-Net_2 (c) Prediction of our developed method.

CONCLUSION

To improve patients' quality of life, we have developed a fully automatic brain tumor segmentation method. In this article, we have proposed a method based on deep learning, using deep convolution networks based on the U-Net model. Our method was evaluated on the BRATS 2017 datasets, which contain both HGG and LGG patients. This method provided an efficient and robust segmentation compared to the manually delineated ground truth and showed a maximum dice similarity coefficient of 0.81 for the dataset used.

REFERENCES

[1] J. A. Schwartzbaum, J. L. Fisher, K. D. Aldape, and M. Wrensch, "Epidemiology and molecular pathology of glioma," Nat. Clin. Pract. Neurol., vol. 2, no. 9, pp. 494–503, 2006

[2] M. Beghetti, R. M. Gow, I. Haney, J. Mawson, W. G. Williams, and R. M. Freedom, "Pediatric primary benign cardiac tumors: A 15-year review," Am. Heart J., vol. 134, no. 6, pp. 1107–1114, 1997.

[3] M. Preusser, F. Winkler, M. Valiente, C. Manegold, E. Moyal, G. Widhalm, J.-C. Tonn, and C. Zielinski, "Recent advances in the biology and treatment of brain metastases of non-small cell lung cancer: summary of a multidisciplinary roundtable discussion," ESMO Open, vol. 3, no. 1, p. e000262, 2018.

[4] N. R. Smoll, K. Schaller, and O. P. Gautschi, "Long-term survival of patients with glioblastoma multiforme (GBM)," J. Clin. Neurosci., vol. 20, no. 5, pp. 670–675, 2013.

[5] R. Ramakrishna, A. Hebb, J. Barber, R. Rostomily, and D. Silbergeld, "Outcomes in Reoperated Low-Grade Gliomas," Neurosurgery, vol. 77, no. 2, pp. 175–184, 2015.

[6] Sharma, N., & Aggarwal, L. M. (2010). Automated medical image segmentation techniques. Journal of medical physics/Association of Medical Physicists of India, 35(1), 3.

[7] Masood, S., Sharif, M., Masood, A., Yasmin, M., & Raza, M. (2015). A survey on medical image segmentation. Current Medical Imaging Reviews, 11(1), 3-14.

[8] Norouzi, A., Rahim, M. S. M., Altameem, A., Saba, T., Rad, A. E., Rehman, A., & Uddin, M. (2014). Medical image segmentation methods, algorithms, and applications. *IETE Technical Review*, *31*(3), 199-213.

[9] S. S. and C. S. Pawar, "An Automatic Brain Tumor Detection and Segmentation using Hybrid Method," Int. J. Appl. Inf. Syst., vol. 11, no. 9, pp. 6–11, 2017.

[10] L. Zhao, W. Wu, and J. J. Corso, "Brain Tumor Segmentation Based on GMM and Active Contour Method with a Model-Aware Edge Map," Proc MICCAI-BRATS (Multimodal Brain Tumor Segmentation Challenge), no. 1, pp. 24–27, 2012.

[11] M. Havaei, A. Davy, D. Warde-Farley, A. Biard, A. Courville, Y. Bengio, C. Pal, P. M. Jodoin, and H. Larochelle, "Brain tumor segmentation with Deep Neural Networks," Med. Image Anal., vol. 35, pp. 18–31, 2017.

[12] E. Shelhamer, J. Long, and T. Darrell, "Fully Convolutional Networks for Semantic Segmentation," IEEE Trans. Pattern Anal. Mach. Intell., vol. 39, no. 4, pp. 640–651, 2017.

[13] Ronneberger, O., Fischer, P., & Brox, T. (2015, October). U-net: Convolutional networks for biomedical image segmentation. In International Conference on Medical image computing and computer-assisted intervention (pp. 234-241). Springer, Cham.

[14] Kermi, A., Mahmoudi, I., & Khadir, M. T. (2018, September). Deep Convolutional Neural Networks Using U-Net for Automatic Brain Tumor Segmentation in Multimodal MRI Volumes. In International MICCAI Brainlesion Workshop (pp. 37-48). Springer, Cham.

[15] Dong, H., Yang, G., Liu, F., Mo, Y., & Guo, Y. (2017, July). Automatic brain tumor detection and segmentation using U-Net based fully convolutional networks. In annual conference on medical image understanding and analysis (pp. 506-517). Springer, Cham.

[16] Bauer, S., Wiest, R., Nolte, L. P., & Reyes, M. (2013). A survey of MRI-based medical image analysis for brain tumor studies. Physics in Medicine & Biology, 58(13), R97.

[17] Mazzara, G. P., Velthuizen, R. P., Pearlman, J. L., Greenberg, H. M., & Wagner, H. (2004). Brain tumor target volume determination for radiation treatment planning through automated MRI segmentation. *International Journal of Radiation Oncology* Biology* Physics*, *59*(1), 300-312.

[18] Milletari, F., Navab, N., & Ahmadi, S. A. (2016, October). V-net: Fully convolutional neural networks for volumetric medical image segmentation. In 2016 Fourth International Conference on 3D Vision (3DV) (pp. 565-571). IEEE.

[19] Galleguillos, C., & Belongie, S. (2010). Context based object categorization: A critical survey. *Computer vision and image understanding*, *114*(6), 712-722.

[20] M. Z., . A. A. S., . S. H. S., . A. Z. J., and . A. K., "Brain Tumor Segmentation through Region-based, Supervised and Unsupervised Learning Methods: A Literature Survey Brain Tumor Segmentation through Image Processing Methods: A Literature Survey," J. Biomed. Eng. Med. Imaging, vol. 6, no. 2, 2019.

[21] Al-Dmour, H., & Al-Ani, A. (2016, December). MR brain image segmentation based on unsupervised and semi-supervised fuzzy clustering methods. In 2016 international conference on digital image computing: techniques and applications (DICTA) (pp. 1-7). IEEE.-47.

[22] Srinivas, B., & Rao, G. S. (2018, January). Unsupervised learning algorithms for MRI brain tumor segmentation. In 2018 Conference on Signal Processing And Communication Engineering Systems (SPACES) (pp. 181-184). IEEE.

[23] Szilágyi, L., Lefkovits, L., & Benyo, B. (2015, August). Automatic brain tumor segmentation in multispectral MRI volumes using a fuzzy c-means cascade algorithm. In 2015 12th international conference on fuzzy systems and knowledge discovery (FSKD) (pp. 285-291). IEEE.

[24] Juan-Albarracín, J., Fuster-Garcia, E., Manjon, J. V., Robles, M., Aparici, F., Martí-Bonmatí, L., & Garcia-Gomez, J. M. (2015). Automated glioblastoma segmentation based on a multiparametric structured unsupervised classification. PLoS One, 10(5), e0125143.

[25] Rajendran, A., & Dhanasekaran, R. (2012). Fuzzy clustering and deformable model for tumor segmentation on MRI brain image: a combined approach. Procedia Engineering, 30, 327-333.

[26] Hsieh, T. M., Liu, Y. M., Liao, C. C., Xiao, F., Chiang, I. J., & Wong, J. M. (2011). Automatic segmentation of meningioma from non-contrasted brain MRI integrating fuzzy clustering and region growing. *BMC medical informatics and decision making*, *11*(1), 54.

[27] Subbanna, N., Precup, D., & Arbel, T. (2014). Iterative multilevel MRF leveraging context and voxel information for brain tumour segmentation in MRI. In Proceedings of the IEEE Conference on Computer Vision and Pattern Recognition (pp. 400-405).

[28] Jafari, M., & Kasaei, S. (2011). Automatic brain tissue detection in MRI images using seeded region growing segmentation and neural network classification. Australian Journal of Basic and Applied Sciences, 5(8), 1066-1079.

[29] Pinto, A., Pereira, S., Correia, H., Oliveira, J., Rasteiro, D. M., & Silva, C. A. (2015, August). Brain tumour segmentation based on extremely randomized forest with high-level features. In 2015 37th annual international conference of the IEEE engineering in medicine and biology society (EMBC) (pp. 3037-3040). IEEE.

[30] Soltaninejad, M., Yang, G., Lambrou, T., Allinson, N., Jones, T. L., Barrick, T. R., ... & Ye, X. (2017). Automated brain tumour detection and segmentation using superpixel-based extremely randomized trees in FLAIR MRI. International journal of computer assisted radiology and surgery, 12(2), 183-203.

[31] Wu, W., Chen, A. Y., Zhao, L., & Corso, J. J. (2014). Brain tumor detection and segmentation in a CRF (conditional random fields) framework with pixel-pairwise affinity and superpixel-level features. International journal of computer assisted radiology and surgery, 9(2), 241-253.

[32] Bonte, S., Goethals, I., & Van Holen, R. (2018). Machine learning based brain tumour segmentation on limited data using local texture and abnormality. Computers in biology and medicine, 98, 39-47.

[33] Litjens, G., Kooi, T., Bejnordi, B. E., Setio, A. A. A., Ciompi, F., Ghafoorian, M., ... & Sánchez, C. I. (2017). A survey on deep learning in medical image analysis. Medical image analysis, 42, 60-88.

[34] Simonyan, K., & Zisserman, A. (2014). Very deep convolutional networks for large-scale image recognition. arXiv preprint arXiv:1409.1556.

[35] Milletari, F., Navab, N., & Ahmadi, S. A. (2016, October). V-net: Fully convolutional neural networks for volumetric medical image segmentation. In 2016 Fourth International Conference on 3D Vision (3DV) (pp. 565-571). IEEE.

[36] Badrinarayanan, V., Kendall, A., & Cipolla, R. (2017). Segnet: A deep convolutional encoder-decoder architecture for image segmentation. IEEE transactions on pattern analysis and machine intelligence, 39(12), 2481-2495.

[37] Han, S., Mao, H., & Dally, W. J. (2015). Deep compression: Compressing deep neural networks with pruning, trained quantization and huffman coding. *arXiv preprint arXiv:1510.00149*.

[38] Menze, B. H., Jakab, A., Bauer, S., Kalpathy-Cramer, J., Farahani, K., Kirby, J., ... & Lanczi, L. (2014). The multimodal brain tumor image segmentation benchmark (BRATS). IEEE transactions on medical imaging, 34(10), 1993-2024.

[39] Bakas, S., Akbari, H., Sotiras, A., Bilello, M., Rozycki, M., Kirby, J. S., ... & Davatzikos, C. (2017). Advancing the cancer genome atlas glioma MRI collections with expert segmentation labels and radiomic features. Scientific data, 4, 170117.

[40] Bakas, S., Reyes, M., Jakab, A., Bauer, S., Rempfler, M., Crimi, A., ... & Prastawa, M. (2018). Identifying the best machine learning algorithms for brain tumor segmentation, progression assessment, and overall survival prediction in the BRATS challenge. arXiv preprint arXiv:1811.02629.

[41] Jones, T. L., Byrnes, T. J., Yang, G., Howe, F. A., Bell, B. A., & Barrick, T. R. (2014). Brain tumor classification using the diffusion tensor image segmentation (D-SEG) technique. Neuro-oncology, 17(3), 466-476.

[42] Kingma, D. P., & Ba, J. (2014). Adam: A method for stochastic optimization. arXiv preprint arXiv:1412.6980.

[43] Kamnitsas, K., Ledig, C., Newcombe, V. F., Simpson, J. P., Kane, A. D., Menon, D. K., ... & Glocker, B. (2017). Efficient multi-scale 3D CNN with fully connected CRF for accurate brain lesion segmentation. *Medical image analysis*, *36*, 61-78.

[44] Pereira, S., Pinto, A., Alves, V., & Silva, C. A. (2016). Brain tumor segmentation using convolutional neural networks in MRI images. *IEEE transactions on medical imaging*, *35*(5), 1240-1251.